MOLECULAR AND CELLULAR BIOLOGY, Mar. 2007, p. 2189–2201 Vol. 27, No. 6
0270-7306/07/$08.00+0 doi:10.1128/MCB.01763-06

Genome Maintenance Defects in Cultured Cells and Mice following Partial Inactivation of the Essential Cell Cycle Checkpoint Gene *Hus1*[▽]

Peter S. Levitt, Min Zhu, Amy Cassano, Stephanie A. Yazinski, Houchun Liu, Joshua Darfler, Rachel M. Peters, and Robert S. Weiss*

Department of Biomedical Sciences, Cornell University, Ithaca, New York 14853

Received 18 September 2006/Returned for modification 11 October 2006/Accepted 20 December 2006

Cell cycle checkpoints are evolutionarily conserved signaling pathways that uphold genomic integrity. Complete inactivation of the mouse checkpoint gene *Hus1* results in chromosomal instability, genotoxin hypersensitivity, and embryonic lethality. To determine the functional consequences of partial Hus1 impairment, we generated an allelic series in which *Hus1* expression was incrementally reduced by combining a hypomorphic *Hus1* allele, $Hus1^{neo}$, with either wild-type or null ($Hus1^{\Delta 1}$) alleles. Primary $Hus1^{neo/\Delta 1}$ embryonic fibroblasts exhibited spontaneous chromosomal abnormalities and underwent premature senescence, while higher *Hus1* expression in $Hus1^{neo/neo}$ cells allowed for normal proliferation. Antioxidant treatment almost fully suppressed premature senescence in $Hus1^{neo/\Delta 1}$ cultures, suggesting a critical role for Hus1 in oxidative stress responses. Treatment of $Hus1^{neo/neo}$ and $Hus1^{neo/\Delta 1}$ cells with the DNA adducting agent benzo(a)pyrene dihydrodriol epoxide resulted in a loss of cell viability that was associated with S-phase DNA damage checkpoint failure. Likewise, the DNA polymerase inhibitor aphidicolin triggered increased cell death, chromosomal aberrations, and H2AX phosphorylation, a marker for double-stranded DNA breaks, in $Hus1^{neo/neo}$ and $Hus1^{neo/\Delta 1}$ cultures compared to controls. Despite these pronounced genome maintenance defects in cultured $Hus1^{neo/\Delta 1}$ and $Hus1^{neo/neo}$ cells, mice of the same genotypes were born at expected frequencies and appeared grossly normal. A significant increase in micronucleus formation was observed in peripheral blood cells from $Hus1^{neo/\Delta 1}$ mice, but reduced *Hus1* expression did not cause an elevated predisposition to spontaneous tumor development or accelerate tumorigenesis in *p53*-deficient mice. These results identify differential effects of altered *Hus1* gene dosage on genome maintenance during in vitro culture, genotoxic stress responses, embryonic development, and adult homeostasis.

The ability to accurately duplicate the genome and correctly segregate damage-free chromosomes to daughter cells is crucial to the health and longevity of all organisms. To ensure the fidelity of these processes, cells respond to genome damage by arresting the cell cycle, stabilizing replication forks, and inducing DNA repair. Cell cycle checkpoint pathways mediate these DNA damage responses and additionally can induce apoptosis if the damage is beyond repair. By preventing the accumulation of mutations that drives carcinogenesis, checkpoints can be important tumor suppressor mechanisms (3, 21, 27).

Replication inhibitors and bulky DNA lesions activate a checkpoint pathway headed by the phosphatidylinositol kinase-like protein kinase Atr. Stalling of replication forks or processing of DNA lesions causes accumulation of single-stranded DNA that becomes coated with replication protein A (RPA) and attracts Atr in association with its binding partner Atrip (12). Atr then transmits the checkpoint signal by phosphorylating Chk1, Brca1, and other targets, which in turn regulate the cell cycle, replication, and repair machineries. Efficient DNA damage signaling through Atr also requires several accessory factors, including TopBP1/Cut5, Claspin, and the Rad9-Rad1-Hus1 (9-1-1) complex (44).

With predicted structural similarity to proliferating cell nuclear antigen (PCNA), the 9-1-1 complex is believed to function as a checkpoint sliding clamp and molecular scaffold (57). Loading of the 9-1-1 trimer onto chromatin is stimulated by genotoxic stress and is mediated by a clamp loader composed of Rad17 and associated replication factor C subunits (8, 41, 67). Once on chromatin, the 9-1-1 complex participates in DNA damage signaling, promoting phosphorylation of Atr substrates such as Chk1, Rad17, and Rad9 itself (2, 40, 65, 67). Signaling defects in cells lacking 9-1-1 components are associated with failure of an S-phase checkpoint that represses late origin firing in response to DNA damage (2, 40, 64). The mammalian 9-1-1 complex also directly associates with a number of DNA repair proteins, including factors involved in base excision repair (10, 20, 46, 48, 55, 58, 59) and translesion DNA synthesis (26, 42), and additionally is required for homologous recombinational repair (37, 61) as well as telomere maintenance (19, 37). Given these key roles in checkpoint signaling and DNA repair, it is not surprising that cells defective for 9-1-1 function are hypersensitive to a wide variety of genotoxins, including replication inhibitors and DNA damaging agents (23, 28, 40, 60, 61, 63, 64).

The mammalian 9-1-1 complex not only responds to extrinsic stresses but also is required for embryonic development. Targeted inactivation of mouse *Hus1* (63) or *Rad9* (23) results

* Corresponding author. Mailing address: Department of Biomedical Sciences, Cornell University, T2-006C Veterinary Research Tower, Ithaca, NY 14853. Phone: (607) 253-4443. Fax: (607) 253-4212. E-mail: rsw26@cornell.edu.

▽ Published ahead of print on 12 January 2007.

in widespread cell death and midgestational embryonic lethality. *Rad17* is also essential for murine embryogenesis (7). Loss of *Atr* (6, 14) or *Chk1* (31, 51) has even more severe consequences and causes peri-implantation lethality. In all of these mouse models, embryonic lethality is associated with spontaneous chromosomal instability, indicating that these gene products are essential for genome maintenance during normal cell proliferation. Even in the absence of extrinsic stresses, mammalian checkpoints regulate Cdc25A turnover (50), the timing of origin firing (45), and replication fork progression through fragile sites in the genome (11).

The analysis of hypomorphic alleles that are partially impaired for gene function is a traditional genetic strategy that can yield important insights into the activity of a given gene. This approach is particularly appropriate for study of the Atr-dependent checkpoint pathway, as its complete inactivation causes severe phenotypes. Moreover, understanding the impact of partial impairment of this essential checkpoint mechanism has significant biomedical implications. For instance, a hypomorphic *ATR* mutation is known to cause the human developmental disorder Seckel syndrome (36). Furthermore, components of this pathway have been suggested to represent a new class of tumor suppressors that may be only partially inactivated in cancers (31). Here, we describe a new mouse model based on a hypomorphic *Hus1* allele that expresses reduced levels of wild-type *Hus1*. Partial reduction of *Hus1* expression in cultured cells was found to cause premature senescence, spontaneous chromosomal abnormalities, and DNA damage hypersensitivity. Unexpectedly, mice with the same genetic alteration were born at the predicted frequency and, despite indications of genomic instability, developed normally without heightened tumor predisposition.

MATERIALS AND METHODS

Mouse strains. Previously described $Hus1^{neo}$ and $Hus1^{\Delta 1}$ mouse strains were maintained on a 129S6 inbred genetic background (30, 63). $Trp53^{tm1Tyj}$ mice were maintained on a C57BL/6 inbred genetic background (25). All mice were housed in accordance with institutional animal care and use guidelines. For analysis of tumor cohorts, animals were aged until they showed clinical signs of disease. Tumors identified grossly at necropsy were fixed in 10% neutral-buffered formalin, embedded in paraffin, sectioned, and stained with hematoxylin and eosin. Histopathological evaluations and tumor classifications were performed blind with respect to genotype. Kaplan Meier survival curves were generated and compared by log rank test using SPSS statistical software.

Cell culture, proliferation measurements, and genotoxin survival assays. Mouse embryonic fibroblasts (MEFs) were generated from 13.5-dpc embryos from timed matings between $Hus1^{+/neo}$ and $Hus1^{+/\Delta 1}$ mice or $Hus1^{+/neo}$ and $Hus1^{neo/\Delta 1}$ mice. Briefly, following removal of the heart, liver, and head, embryos were mechanically disaggregated and the resulting single-cell suspension was cultured in culture medium (Dulbecco minimal essential medium [DMEM] supplemented with 10% fetal bovine serum, 1.0 mM L-glutamine, 0.1 mM MEM nonessential amino acids, 100 μg/ml of streptomycin sulfate, and 100 U/ml of penicillin). Serial MEF cultures were maintained according to the 3T3 protocol in which 10^6 cells were passaged onto 10-cm dishes every 3 days (54). The initial plating was considered passage zero. When primary cultures entered senescence, the cells were provided fresh culture medium but passaged only upon reaching confluence, until immortalized clones emerged. Population doublings were calculated with the formula $\Delta PDL = \log(n_f/n_o)/\log_2$, where n_o is the initial number of cells and n_f is the final number of cells (4). The effect of antioxidant treatment was assessed by culturing cells beginning at passage one in culture medium containing 5 mM *N*-acetyl-alanine (NAA) (Sigma) or *N*-acetyl-cysteine (NAC) (Sigma), which was changed daily. For short-term proliferation assays, 10^5 cells were plated per six-well dish well and, at 24-h intervals, triplicate samples were harvested by trypsinization. The number of viable cells in individual samples was determined after incubation with trypan blue dye. For short-term genotoxin survival assays, 10^5 cells were plated per six-well dish well, treated with genotoxin, cultured for 3 days, and then harvested by trypsinization, incubated with trypan blue dye, and individually counted. For benzo(a)pyrene dihydrodriol epoxide (BPDE) (NCI carcinogen repository) treatment, the genotoxin was added directly to the medium and cells were then incubated for 1 h, after which time the genotoxin-containing medium was removed, cells were washed once with phosphate-buffered saline (PBS), and fresh medium was added. Treatments with aphidicolin (Sigma) were done similarly, except that genotoxin exposure to cells was for 24 h.

Radioresistant DNA synthesis assay. Cells were plated in triplicate at a density of 2×10^5 per well of a gelatinized six-well dish. The next day, the cells were treated with BPDE for 1 h, washed with PBS, incubated for 30 min in culture medium without genotoxin, and labeled for 1 h in medium containing 2.5 μCi/ml *methyl*-[^{3}H]thymidine (2.0 Ci/mmol; NEN Life Science Products, Inc). The radioactive medium was then removed, and unincorporated nucleotides were removed by washing the cells three times in ice-cold 5.0% trichloroacetic acid. The cells were then solubilized in 0.3 N NaOH, followed by neutralization with glacial acetic acid. Radioactivity was quantitated with a liquid scintillation counter.

Northern blot hybridization and reverse transcriptase (RT) PCR. Total RNA was prepared from passage-one MEF cultures with RNA STAT-60 reagent (Tel-Test). Northern blot hybridization was performed as described previously (63). The signal intensity for wild-type *Hus1* transcripts was determined by phosphorimager and normalized to the signal intensity for *Gapdh* for the same RNA sample. cDNA was prepared from 3 μg of DNase-treated RNA by random priming with the SuperScript preamplification system (Gibco BRL). PCR amplification was performed with the following primers (see also Fig. 2): 1 (5′ BamH1), 5′-CTCGGATCCATGAAGTTTCGCGCCAAG-3′; 2 (3′ EcoRI), 5′-CTCGAATTCCTAGGACAAGGCTGGGAT-3′; 3 (3.224), 5′-TCTTCAGA GACTCCTTCCATT-3′; 4 (Neo2), 5′-TTCGTCCAGATCATCCTGATC-3′; 5 (Neo1), 5′-AGAGGCTATTCGGCTATGACTG-3′; 6 (Neo 3′), 5′-GGTATCG CCGCTCCCGATTCGCAG-3′. PCR products generated with primers 1 and 2 were digested with BamHI and EcoRI and cloned into pBluescript II (Stratagene). All other PCR products were cloned into vector pCR2.1 by TOPO TA cloning (Invitrogen). cDNA inserts were fully sequenced.

Metaphase spread preparation. MEFs were incubated in culture medium containing 0.15 μg/ml Colcemid for 1 h. Cells were then harvested by trypsinization, swollen for 12 min at 37°C in hypotonic buffer (0.034 M KCl, 0.017 M $Na_3C_6H_5O_7$), and fixed for at least 20 min at 4°C in 75% methanol–25% acetic acid. Cells in fixative were then spotted onto microscope slides and stained with 2.0% Giemsa in Gurr buffer (pH 6.8). Chromosomal abnormalities were scored based on standard guidelines (34, 43). For analysis of aphidicolin-induced chromosomal abnormalities, MEFs were treated with 0.05 μM or 0.10 μM aphidicolin for 24 h and then immediately subjected to metaphase spread preparation as described above.

Indirect immunofluorescence. Cells grown on glass slides were fixed with 2% paraformaldehyde in Tris-buffered saline (TBS) for 35 min at 4°C. The cells were then permeabilized and blocked with 3% bovine serum albumin, 0.2% TritonX-100, and 0.01% nonfat dried milk in TBS for 20 min at room temperature. Cells were incubated sequentially with primary anti-γ-H2AX antibody (JBW301; Upstate) at 1:500 for 45 min, secondary goat anti-mouse immunoglobulin G (H+L)-fluorescein isothiocyanate (FITC) (Southern Biotechnology) at 1:60 for 35 min, and DAPI (4′,6′-diamidino-2-phenylindole) (33 ng/ml) for 1 min. Slides were viewed with a Leica DMRE fluorescence microscope.

Micronucleus assay. Analysis of micronucleus formation in peripheral blood cells was performed as described by others (39). Briefly, 50 μl of peripheral blood was collected from the mandibular vein into a microcentrifuge tube containing 200 μl of heparin solution (500 USP heparin/ml PBS) and fixed in methanol at −80°C overnight. After washing with ice-cold bicarbonate buffer (0.9% NaCl, 5.3 mM $NaHCO_3$ [pH 7.5]), the cells were incubated in bicarbonate buffer containing RNase A and anti-CD71:FITC antibody (Biodesign International) at 4°C for 45 min. The samples were then washed with bicarbonate buffer, resuspended in propidium iodide (1.25 μg/ml in bicarbonate buffer), and analyzed on a FACSCalibur flow cytometer (Becton-Dickinson, San Jose, CA) as described by others (15).

RESULTS

***Hus1^{neo}* is a hypomorphic allele that expresses a reduced level of wild-type *Hus1*.** In the process of producing a *loxP* site-flanked conditional *Hus1* allele, $Hus1^{flox}$ (30), we generated the $Hus1^{neo}$ allele, which contains a *frt*-flanked *neo* cassette in intron one as well as *loxP* sites surrounding exons two

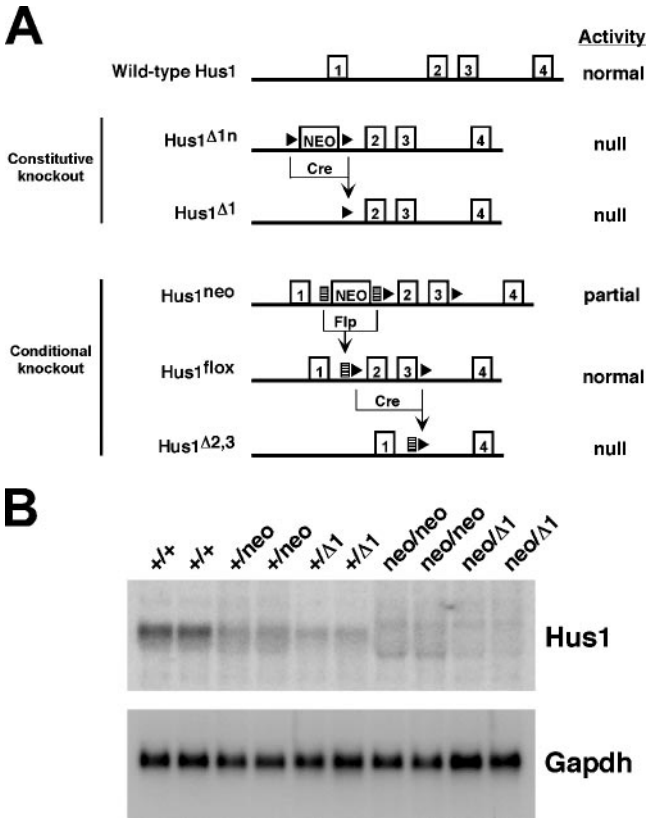

FIG. 1. *Hus1* allelic series. (A) Schematic representation of the *Hus1* alleles generated in systems for constitutive and conditional *Hus1* inactivation. The first four *Hus1* exons are shown as boxed numbers. A neomycin resistance cassette (NEO), *frt* sites (lined rectangles), and *loxP* sites (solid triangles) are shown. Exposure of alleles containing *frt* sites to the Flp recombinase or alleles containing *loxP* sites to the Cre recombinase excises the intervening sequence, generating a new allele as indicated. (B) Northern blot analysis of primary MEF cultures. Total RNA was prepared from individual MEF cultures of the indicated genotypes and hybridized with a ^{32}P-labeled *Hus1* or *Gapdh* cDNA probe. RNA prepared from each MEF culture was loaded in duplicate.

and three (Fig. 1A). Often the presence of a *neo* cassette in a targeted gene interferes with the expression of that gene (29). Given that complete *Hus1* inactivation results in embryonic lethality and severe proliferation defects in cultured cells, we reasoned that a reduced level of *Hus1* expression from the $Hus1^{neo}$ allele might be useful for testing the impact of a partial impairment of this essential checkpoint gene. Therefore, we used $Hus1^{neo}$, in combination with wild-type *Hus1* and the previously described null $Hus1^{\Delta 1}$ allele (63), to produce a *Hus1* allelic series (Fig. 1A). MEFs of all possible genotypes except $Hus1^{\Delta 1/\Delta 1}$ were generated. $Hus1^{\Delta 1/\Delta 1}$ MEFs cannot be produced because of the early embryonic lethality associated with this genotype (63). Northern blot analysis revealed a striking incremental reduction in *Hus1* expression through the series (Fig. 1B). The graded pattern of *Hus1* expression observed ($Hus1^{+/+} > Hus1^{+/neo} > Hus1^{+/\Delta 1} > Hus1^{neo/neo} > Hus1^{neo/\Delta 1}$) suggested that $Hus1^{neo}$ produced a significantly reduced level of *Hus1*. Quantification of the Northern blot signal by phosphorimager analysis indicated each $Hus1^{neo}$ allele expressed roughly 40% of the wild-type level of *Hus1* ($Hus1^{+/+}$, 100%; $Hus1^{+/neo}$, 71.4%; $Hus1^{+/\Delta 1}$, 43.5%; $Hus1^{neo/neo}$, 47.4%; $Hus1^{neo/\Delta 1}$, 20.8%).

Examination of the Northern blot signal for $Hus1^{neo/neo}$ samples suggested the presence of wild-type *Hus1* transcripts as well as novel RNA species, including both larger and smaller transcripts. Therefore, a thorough analysis of *Hus1* expression from $Hus1^{neo}$ was performed by RT-PCR (Fig. 2). Control reactions from which RT was omitted did not yield detectable PCR products, confirming the absence of contaminating genomic DNA (Fig. 2A and data not shown). $Hus1^{neo}$ contains all wild-type *Hus1* sequences and, as expected, produced wild-type *Hus1* transcripts (Fig. 2A). Although these RT-PCR assays are not quantitative, a reduced amount of wild-type *Hus1* product was amplified from $Hus1^{neo/neo}$ cells compared to $Hus1^{+/+}$ cells, consistent with the results of the Northern blot analysis. The presence of the *neo* cassette also induced skipping of exons two and three with increased frequency. Due to a frameshift, the resulting transcript in which exon one is spliced to exon four has the capacity to encode only the first 19 Hus1 amino acids and is functionally inactive (30). The *neo* cassette used in this study is reported to contain cryptic splice acceptor and donor sites (33), and accordingly some $Hus1^{neo}$ transcripts also spliced from *Hus1* sequences into the *neo* cassette. Other $Hus1^{neo}$ transcripts appeared to originate from within the *neo* cassette and then spliced into *Hus1* sequences (Fig. 2B). Unfortunately, endogenous mouse Hus1 protein could not be detected from primary MEFs with the available antibody reagents, and it was not possible to characterize Hus1 expression from $Hus1^{neo}$ in this manner. However, all aberrant transcripts produced from $Hus1^{neo}$ contained premature stop codons and had the capacity to produce only highly truncated protein fragments containing little Hus1 sequence. As detailed below, $Hus1^{+/neo}$ cells and mice were completely normal in all assays in which they were tested, indicating that $Hus1^{neo}$ has no detectable dominant activities, although we cannot rule out subtle effects due to the production of aberrant transcripts from this allele. Together, these results indicate that $Hus1^{neo}$ is a hypomorphic allele that expresses a reduced level of wild-type *Hus1*.

Partial reduction of *Hus1* expression in cultured cells results in proliferation defects and spontaneous chromosomal abnormalities. Although the gross morphology of embryos of all genotypes in the allelic series was indistinguishable, $Hus1^{neo/\Delta 1}$ fibroblasts appeared to grow poorly once in culture. To quantify these observations, we initially performed short-term proliferation assays with MEFs at passage three. $Hus1^{neo/\Delta 1}$ MEFs showed a severely limited growth capacity compared to control $Hus1^{+/+}$ MEFs (Fig. 3A). $Hus1^{neo/neo}$ MEFs, on the other hand, grew as well as $Hus1^{+/+}$ cells (Fig. 3B). $Hus1^{+/neo}$ and $Hus1^{+/\Delta 1}$ MEFs also showed normal growth (data not shown). The impaired growth of $Hus1^{neo/\Delta 1}$ MEFs observed in these short-term assays prompted us to examine the growth capacity of these cells over a longer time frame. $Hus1^{+/+}$, $Hus1^{neo/neo}$, and $Hus1^{neo/\Delta 1}$ MEFs were cultured according to the 3T3 protocol (54), and cumulative population doublings were calculated. When cultured in this manner, primary mouse fibroblasts typically grow rapidly for 5 to 10 passages before undergoing growth arrest, a process termed senescence. Later, highly proliferative immortalized clones emerge spontaneously. As shown in Fig. 3C, MEFs of all *Hus1*

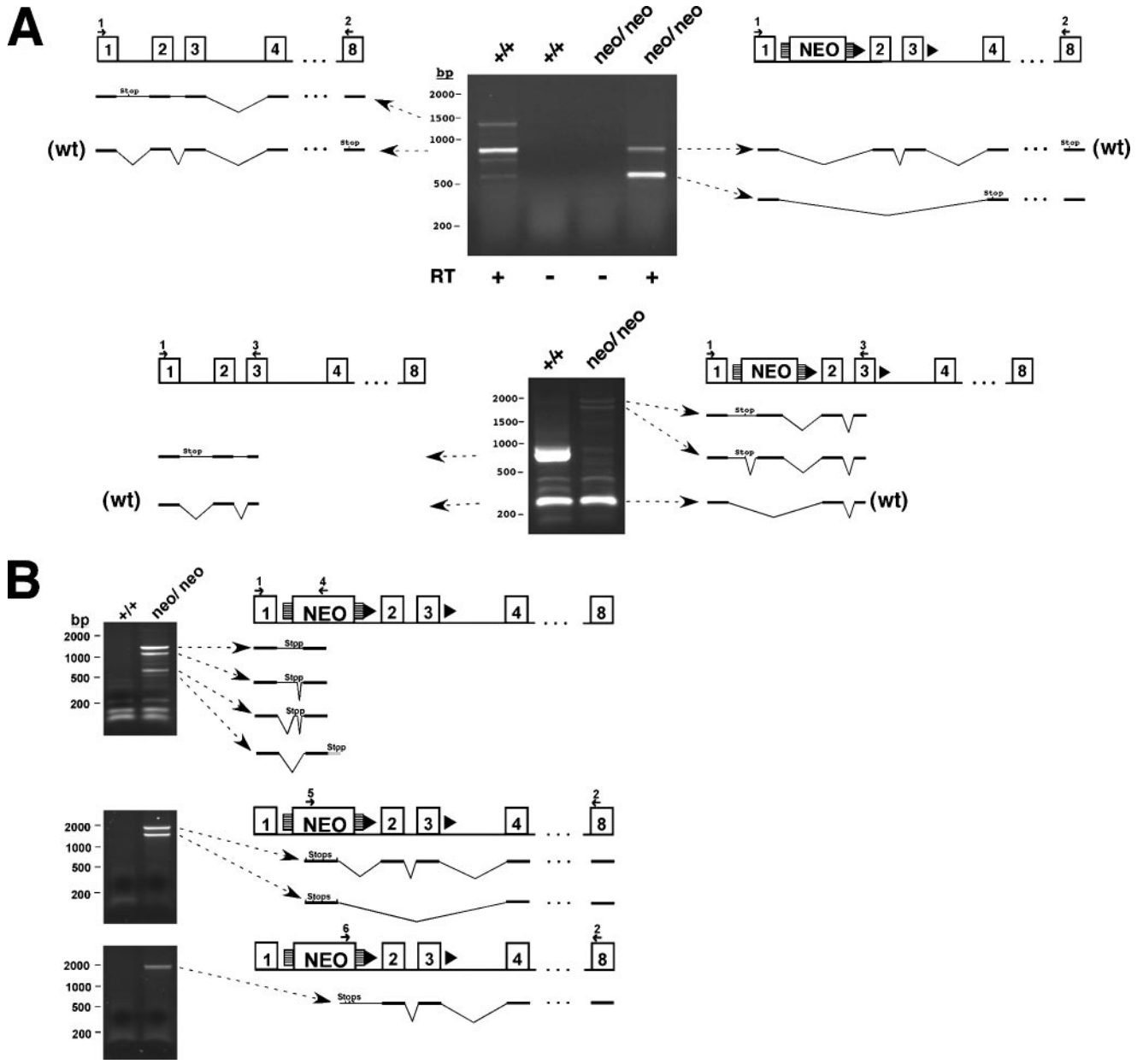

FIG. 2. *Hus1*^{neo} expresses both wild-type and aberrant noncoding transcripts. DNase-treated total RNA from MEFs of the indicated genotypes was reverse transcribed and subjected to PCR analysis using either two *Hus1*-specific primers (A) or one *Hus1*-specific and one *neo*-specific primer (B). Control reactions were performed in the absence of RT as indicated. Primer locations are indicated and correspond to the sequences listed in Materials and Methods. The resulting cDNAs were cloned and sequenced, and the structure of each transcript is diagrammed. Note that *Hus1* transcripts from the wild-type allele often show retention of introns one and/or two. In-frame stop codons are indicated for transcripts originating in *Hus1* coding sequences. In panel B, the smallest of the sequenced PCR products generated by primers 1 plus 4 does not contain an in-frame stop codon. For this cDNA, predicted sequence adjacent to the PCR product is depicted in gray and includes an in-frame stop codon. Stop codons for all three reading frames are indicated for transcripts originating in the *neo* cassette.

genotypes proliferated to similar extents for the first 3 to 6 days in culture. However, *Hus1*$^{neo/\Delta 1}$ MEFs then underwent a premature growth arrest, ceasing proliferation at an earlier passage than *Hus1*$^{+/+}$ or *Hus1*$^{neo/neo}$ MEFs. Eventually, cells of all three genotypes, including *Hus1*$^{neo/\Delta 1}$, became immortalized and resumed rapid growth.

The senescence of MEFs is believed to be a response to extrinsic cellular stresses. In particular, cells cultured under standard conditions experience high, nonphysiological oxygen levels, and the resulting oxidative DNA damage is a primary driving force for senescence in MEFs (38). We hypothesized that the premature senescence of *Hus1*$^{neo/\Delta 1}$ MEFs might be due to a heightened sensitivity to oxidative stress, as Hus1 associates with several base excision repair proteins that promote the repair of oxidative lesions (10, 20, 46, 48, 55, 58, 59). Therefore, we tested the impact of the antioxidant NAC on the

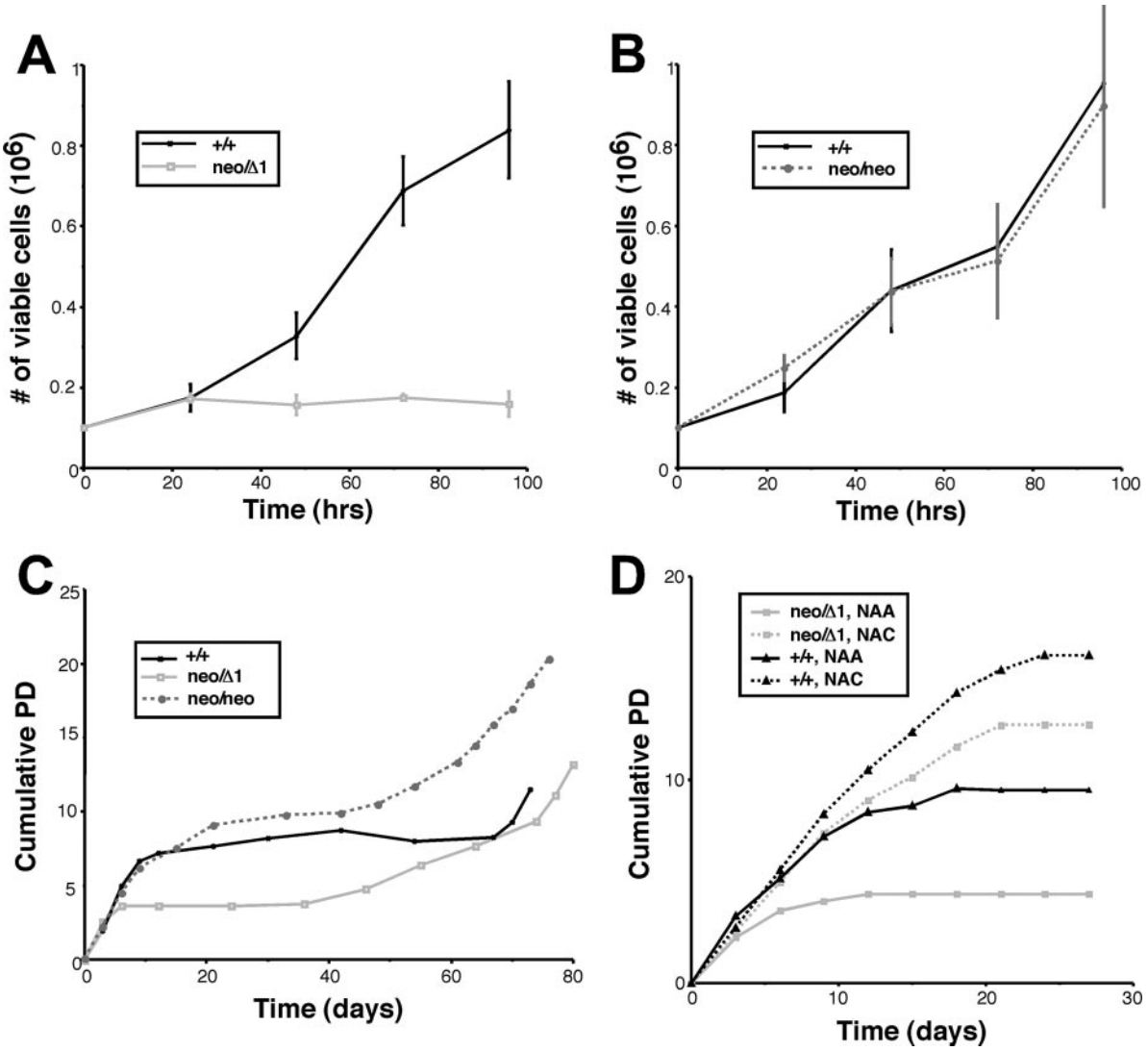

FIG. 3. Impaired proliferation of cells expressing reduced levels of *Hus1*. (A and B) Short-term proliferation of $Hus1^{neo/\Delta 1}$ and $Hus1^{neo/neo}$ MEFs along with matched $Hus1^{+/+}$ control cells. MEF cultures at passage three were seeded into six-well dishes in triplicate, and the number of viable cells was determined at the indicated times postplating. Plots show the mean, with error bars representing the standard deviation. (C) Long-term proliferation of $Hus1^{+/+}$, $Hus1^{neo/neo}$, and $Hus1^{neo/\Delta 1}$ cells. Cumulative population doublings were calculated for MEF cultures of the indicated genotypes maintained according to a 3T3 passaging protocol, as described in Materials and Methods. (D) Effects of antioxidant treatment on the proliferation of $Hus1^{+/+}$ and $Hus1^{neo/\Delta 1}$ cells. $Hus1^{+/+}$ and $Hus1^{neo/\Delta 1}$ MEFs were cultured in culture medium containing 5 mM NAA or NAC, which was changed daily. Cumulative population doublings were calculated as described for panel C.

growth of $Hus1^{+/+}$ and $Hus1^{neo/\Delta 1}$ MEFs (Fig. 3D). Cells treated with the control compound NAA behaved in the same manner as the untreated cells described above, with $Hus1^{neo/\Delta 1}$ cultures undergoing a proliferative arrest much earlier than their $Hus1^{+/+}$ counterparts. Remarkably, treatment with the antioxidant NAC nearly fully suppressed the premature senescence of $Hus1^{neo/\Delta 1}$ MEFs. Although NAC also permitted sustained proliferation of $Hus1^{+/+}$ MEFs at later time points, it significantly enhanced the proliferation of $Hus1^{neo/\Delta 1}$ MEFs at early time points, several passages before it had any detectable effect on $Hus1^{+/+}$ cells, suggesting that premature senescence in $Hus1^{neo/\Delta 1}$ MEFs is due at least in part to an impaired response to oxidative stress.

We next assessed whether the poor growth and premature senescence shown by $Hus1^{neo/\Delta 1}$ MEFs was associated with genomic instability. Metaphase spreads were prepared from MEFs of each genotype in the allelic series at passages one through three, and gross chromosomal abnormalities were scored (Fig. 4A). At passage one, an increased percentage of $Hus1^{neo/\Delta 1}$ metaphases had chromosomal aberrations compared to all other genotypes. The increase in chromosomal abnormalities in $Hus1^{neo/\Delta 1}$ cells was even greater at passage two, and by passage three 48% of $Hus1^{neo/\Delta 1}$ MEFs had at least one chromosomal abnormality and 32% had multiple abnormalities. By contrast, 84% of $Hus1^{+/+}$ metaphases were normal at passage three, and only 9% had multiple abnormalities. $Hus1^{neo/neo}$ MEFs showed an intermediate level of chromosomal instability which was not apparent until later passages.

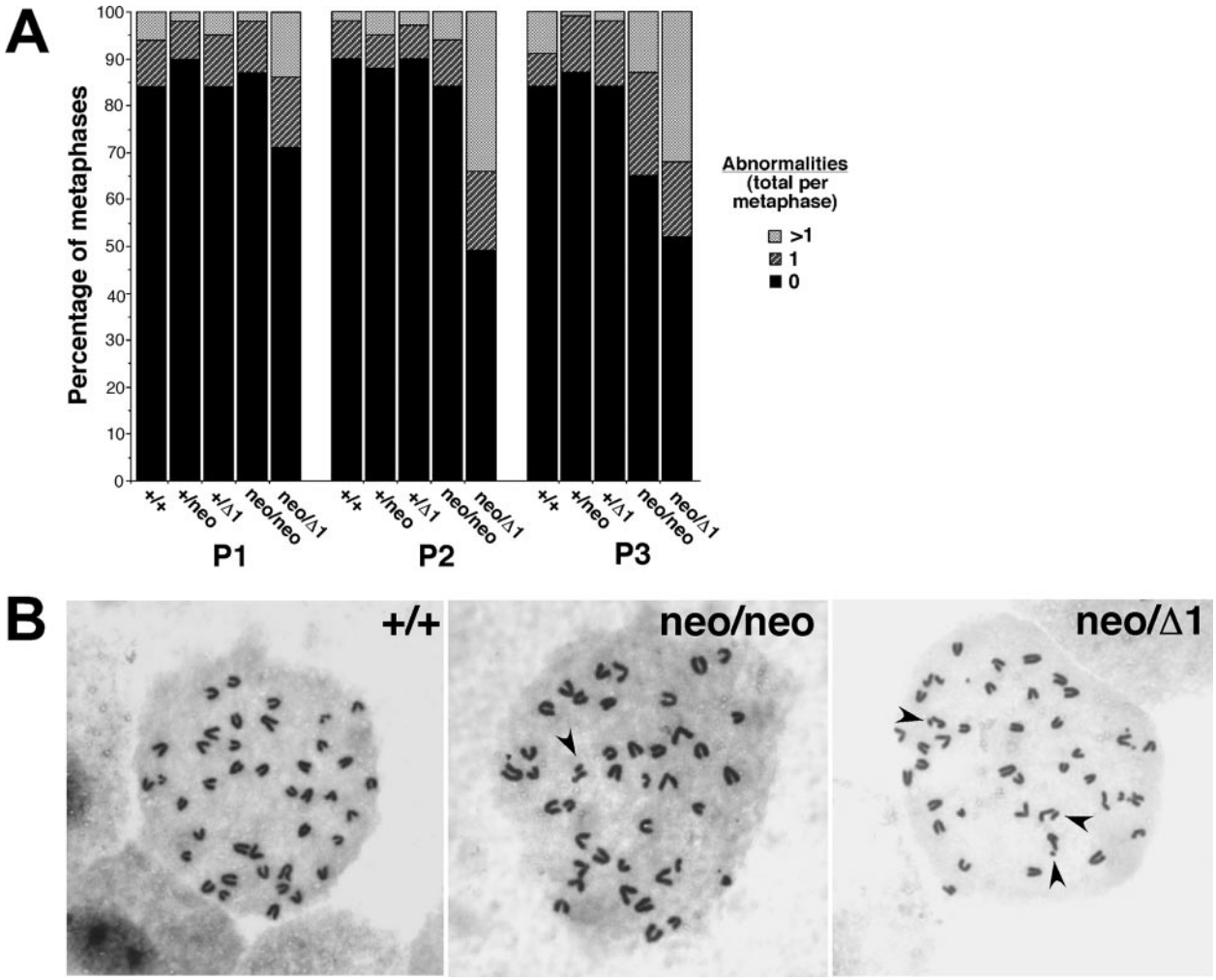

FIG. 4. A partial reduction in *Hus1* expression results in chromosomal instability. (A) Summary of the frequency of chromosomal abnormalities in MEFs with reduced *Hus1* expression. A total of 60 to 93 metaphases, prepared from at least three independent MEF cultures, were scored for each genotype at each passage. (B) Representative metaphase spreads from primary cultures expressing reduced levels of *Hus1*. Metaphase spreads were prepared from $Hus1^{+/+}$, $Hus1^{neo/neo}$, and $Hus1^{neo/\Delta 1}$ MEFs at passage three and stained with Giemsa. Arrows highlight some of the chromosomal abnormalities.

By passage three, 35% of $Hus1^{neo/neo}$ metaphases contained at least one chromosomal abnormality and 13% contained multiple abnormalities. As reported previously for primary *Hus1*-null MEFs (63), the chromosomal abnormalities in $Hus1^{neo/\Delta 1}$ MEFs were primarily chromatid gaps and breaks, and the relative frequency for different types of chromosomal lesions was similar for all genotypes (data not shown; see also Table 1). Representative metaphases are shown in Fig. 4B. Together, these data indicate that a partial reduction in *Hus1* expression leads to spontaneous chromosomal abnormalities that accumulate over time and are associated with premature cellular senescence.

Cells with partial impairment of *Hus1* expression are hypersensitive to DNA damage and replication stress. Because the level of *Hus1* expressed from $Hus1^{neo}$ was insufficient for genomic stability under normal culture conditions, it was also of interest to test how partial *Hus1* impairment would impact cellular responses to DNA damage or replication blockage. Sensitivity to the bulky DNA lesion-inducing agent BPDE, a genotoxin to which *Hus1*-null cells are hypersensitive (64), was tested in short-term viability assays (Fig. 5A). These assays employed MEFs at passage one, a passage at which untreated cells of all genotypes proliferated similarly (Fig. 3C and data not shown). $Hus1^{neo/\Delta 1}$ MEFs showed a significant increase in BPDE sensitivity. At 72 h after treatment with 150 nM BPDE, only 18.8% ± 6.2% of $Hus1^{neo/\Delta 1}$ cells remained viable, compared to 46.3% ± 2.3% of control $Hus1^{+/\Delta 1}$ cells. Although untreated $Hus1^{neo/neo}$ MEFs proliferated normally, it was of interest to test whether the level of Hus1 expressed in these cells would allow cells to cope with a greater level of genome damage. $Hus1^{neo/neo}$ MEFs showed an intermediate sensitivity to BPDE relative to $Hus1^{+/\Delta 1}$ and $Hus1^{neo/\Delta 1}$ MEFs, with 27.8% ± 5.2% of cells of this genotype surviving treatment with 150 nM BPDE. Additional control experiments indicated that $Hus1^{+/neo}$ and $Hus1^{+/\Delta 1}$ MEFs were as sensitive to BPDE and all other genotoxins tested as $Hus1^{+/+}$ MEFs (data not shown). The BPDE hypersensitivity of cells with a partial reduction in *Hus1* expression was associated with defects in an

TABLE 1. Aphidicolin-induced chromosomal abnormalities in cells with reduced *Hus1* expression[a]

Hus1 genotype	Aphidicolin (μM)	Total no. of metaphases	No. of breaks/gaps				No. of chromatid interchanges		No. with extensive damage[b]
			Chromosome type	Chromatid type	Total	Avg	Total	Avg	
+/*neo*	Untreated	19	0	3	3	0.16	0	0	0
	0.05	20	3	2	5	0.25	0	0	0
	0.1	20	1	11	12	0.6	0	0	0
neo/*neo*	Untreated	20	0	9	9	0.45	3	0.15	0
	0.05	20	0	9	9	0.45	10	0.5	1
	0.1	20	2	19	20	0.95	14	0.7	1
neo/Δ*1*	Untreated	19	0	6	6	0.32	0	0	0
	0.05	19	2	22	24	1.26	15	0.79	0
	0.1	19	0	19	19	1.00	14	0.74	3

[a] MEFs of the indicated *Hus1* genotype were left untreated (control) or treated with the indicated dose of aphidicolin for 24 h. Metaphase spreads were then prepared, and chromosomal abnormalities were scored.
[b] Severely damaged metaphases with too many abnormalities to count.

intra-S DNA damage checkpoint that inhibits DNA synthesis in response to genome damage (Fig. 5B). At 1 h after treatment with 100 nM BPDE, the level of DNA synthesis in $Hus1^{+/\Delta 1}$ MEFs was reduced to 61.9% ± 0.5% of that for untreated control cultures. $Hus1^{neo/neo}$ MEFs showed a slightly greater level of DNA synthesis following BPDE treatment (64.7% ± 0.7% of untreated control levels), but this was not significantly different from the value for $Hus1^{+/\Delta 1}$ cells. However, in BPDE-treated $Hus1^{neo/\Delta 1}$ MEFs, DNA synthesis was maintained at 79.4% ± 2.0% of that for untreated control cultures. Impaired proliferation in untreated $Hus1^{neo/\Delta 1}$ MEFs could lead to an overestimation of the extent of the S-phase checkpoint defect, although similar results were obtained with cells at passage one, when cells of all genotypes proliferate similarly (data not shown). Thus, a partial reduction in *Hus1* expression leads to defective S-phase checkpoint function and increased sensitivity to DNA damage. The results additionally identify a level of Hus1 in $Hus1^{neo/neo}$ MEFs that is sufficient under normal growth conditions but is sublimiting for the response to extrinsic genotoxic stresses.

The response of cells with reduced *Hus1* expression to replication stress was also examined, and *Hus1* expression from $Hus1^{neo}$ was found to be sublimiting for cellular responses to the replication inhibitor aphidicolin (Fig. 5C). In short-term viability assays, $Hus1^{neo/\Delta 1}$ MEFs at passage one showed an approximately fivefold increase in sensitivity to aphidicolin relative to $Hus1^{+/\Delta 1}$ MEFs. $Hus1^{neo/neo}$ MEFs showed intermediate aphidicolin sensitivity. A similar pattern of hypersensitivity was observed when MEFs of the allelic series were treated with hydroxyurea, another inhibitor of DNA synthesis (data not shown).

To gain insights into the basis for increased sensitivity to replication inhibitors in cells with reduced *Hus1* expression, we examined the accumulation of double-strand breaks (DSB) following blockage of DNA synthesis in these cells. For this purpose, we performed immunofluorescence assays to detect γ-H2AX, the phosphorylated form of histone H2AX that marks sites of DSB formation (53). Although Atr is responsible for H2AX phosphorylation in response to replication stress, Hus1 is dispensable for this process (62). As shown in Fig. 5D, reduced *Hus1* expression resulted in an increased frequency of γ-H2AX-positive cells, even in the absence of extrinsic genotoxin. Treatment of these cells with aphidicolin resulted in a substantial increase in γ-H2AX staining. Following low-dose (0.1 μM) aphidicolin treatment, only 1.4% of $Hus1^{+/+}$ MEFs were γ-H2AX positive, while 6.6% and 21.7% of $Hus1^{neo/neo}$ and $Hus1^{neo/\Delta 1}$ MEFs, respectively, were γ-H2AX positive after aphidicolin exposure. Similar results were obtained when γ-H2AX accumulation was analyzed by immunoblotting (data not shown). These results suggest that reduced *Hus1* expression results in accumulation of DSB under conditions of replication stress. To further assess the genomic consequences of blockage of DNA synthesis when *Hus1* levels are sublimiting, we produced metaphase spreads from MEFs of the allelic series after low-dose aphidicolin treatment. As expected, treatment of control $Hus1^{+/neo}$ MEFs with aphidicolin resulted in an increase in the frequency of chromatid-type and chromosome-type gaps and breaks (Table 1). In untreated $Hus1^{neo/neo}$ and $Hus1^{neo/\Delta 1}$ MEFs, there were greater numbers of chromatid gaps and breaks than in $Hus1^{+/neo}$ MEFs, and following aphidicolin treatment the frequency of these lesions, as well as chromosome-type gaps and breaks, increased significantly. Interestingly, the frequency of chromatid interchanges also increased dramatically following aphidicolin treatment in both $Hus1^{neo/neo}$ and $Hus1^{neo/\Delta 1}$ MEFs, but not in control $Hus1^{+/neo}$ MEFs. Representative metaphase spreads are shown in Fig. 5E. These findings indicate that the level of *Hus1* expressed from $Hus1^{neo}$ is inadequate for responding to replication stress, leading to the formation of DSB and aberrant chromosomal structures.

Mice with reduced Hus1 expression are grossly normal despite increased genomic instability. Because MEFs with reduced *Hus1* expression showed premature senescence, spontaneous chromosomal abnormalities, and impaired DNA damage responses, we expected that mice of the corresponding genotypes also would display severe phenotypes. Surprisingly, mice of all genotypes in the allelic series were born at the expected frequency. Intercrosses between $Hus1^{+/neo}$ mice produced $Hus1^{neo/neo}$ animals in an approximately one-in-four ratio (41 $Hus1^{+/+}$/86 $Hus1^{+/neo}$/49 $Hus1^{neo/neo}$). Likewise, ap-

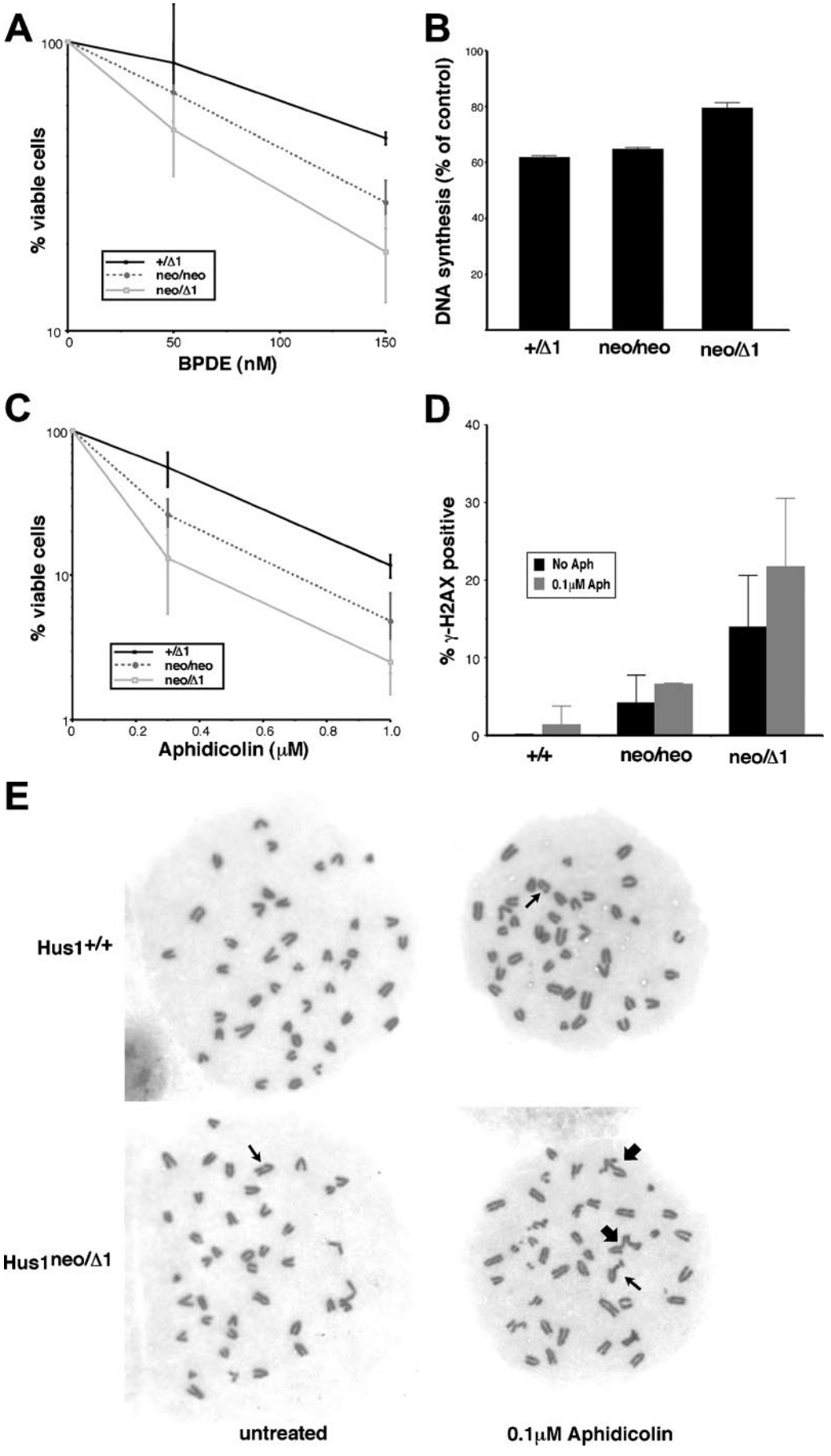
A
100
10
% viable cells
+/Δ1
neo/neo
neo/Δ1
0
50
100
150
BPDE (nM)
B
DNA synthesis (% of control)
100
80
60
40
20
+/Δ1
neo/neo
neo/Δ1
C
100
10
1
% viable cells
+/Δ1
neo/neo
neo/Δ1
0
0.2
0.4
0.6
0.8
1.0
Aphidicolin (μM)
D
% γ-H2AX positive
40
30
20
10
0
No Aph
0.1μM Aph
+/+
neo/neo
neo/Δ1
E
Hus1+/+
Hus1neo/Δ1
untreated
0.1μM Aphidicolin

proximately one-quarter of the offspring from crosses between $Hus1^{+/neo}$ and $Hus1^{+/\Delta 1}$ mice were of the $Hus1^{neo/\Delta 1}$ genotype (61 $Hus1^{+/+}$/69 $Hus1^{+/neo}$/74 $Hus1^{+/\Delta 1}$/65 $Hus1^{neo/\Delta 1}$). $Hus1^{neo/neo}$ and $Hus1^{neo/\Delta 1}$ mice were of normal size and appeared indistinguishable from control littermates. Litters of typical size were produced from three independent matings of adult $Hus1^{neo/\Delta 1}$ mice, indicating that mice of this genotype were fertile.

To test whether reduced *Hus1* expression resulted in genomic instability in vivo, we quantitated the frequency of micronucleus formation in peripheral blood cells from mice of the allelic series. Micronuclei arise from chromosomes that mis-segregate during mitosis or from acentric fragments that are not incorporated into the nucleus (22). Micronucleus formation is a proven indicator of genomic instability and can be induced by genotoxin exposure or by genetic defects, such as mutation of the *Atm* checkpoint gene (47). A flow cytometric assay has been developed to quantify micronucleus formation in peripheral blood cells, based on the fact that maturing reticulocytes expel their main nucleus but not micronuclei (15). Peripheral blood was drawn from mice of the allelic series and stained with anti-CD71 antibody, to distinguish reticulocytes from mature normochromatic erythrocytes, and with propidium iodide, to identify cells with micronuclei (Fig. 6A). In peripheral blood from $Hus1^{+/+}$ mice, the fraction of erythrocytes with micronuclei was 0.12% ± 0.02% on average (Fig. 6B). A similarly low level of micronucleus formation was observed for $Hus1^{+/neo}$, $Hus1^{+/\Delta 1}$, and $Hus1^{neo/neo}$ mice. Notably, a significantly increased fraction of erythrocytes with micronuclei (0.37% ± 0.09%) was observed in peripheral blood from $Hus1^{neo/\Delta 1}$ mice. For clarity, results are shown only for female mice because micronucleus formation is generally lower in female mice than in male mice. A similar proportional increase in micronucleus formation in $Hus1^{neo/\Delta 1}$ mice also was observed in male animals (data not shown). These data indicate that reduced *Hus1* expression results in genomic instability in vivo.

To determine whether increased genomic instability would induce tumor development in mice with a partial *Hus1* impairment, we aged and monitored mice of all genotypes in the allelic series for 14 to 22 months. Overall survival was similar for all genotypes, and no increase in spontaneous tumor development was observed for mice with reduced *Hus1* expression. We therefore tested whether partial *Hus1* inactivation would promote tumorigenesis in combination with a defined oncogenic stimulus. For this purpose, we produced the *Hus1* allelic series in $p53^{-/-}$ and $p53^{+/-}$ genetic backgrounds and examined whether the kinetics of tumor development or the spectrum of tumor types in *p53*-deficient mice would be affected by a partial *Hus1* defect. Consistent with published results (16, 17, 25), $Hus1^{+/+}p53^{-/-}$ mice rapidly lost viability due to tumor development, demonstrating a median survival of 146 days. Reduced *Hus1* gene dosage did not alter the kinetics of tumor development in $p53^{-/-}$ mice, with median survival times of 152, 157, and 149 days observed for $Hus1^{+/neo}p53^{-/-}$, $Hus1^{+/\Delta 1}p53^{-/-}$, and $Hus1^{neo/\Delta 1}p53^{-/-}$ mice, respectively (Fig. 7A) ($P = 0.951$ [log rank test]). Partial *Hus1* impairment also did not affect the spectrum of tumors arising in $p53^{-/-}$ mice (Fig. 7C) ($P = 0.913$ [chi-square test]). Regardless of *Hus1* genotype, the majority of *p53*-null mice developed lymphomas, with most remaining mice developing sarcomas.

Because the strong tumor predisposition in $p53^{-/-}$ mice might mask the impact of partial *Hus1* impairment, we also generated the *Hus1* allelic series in a $p53^{+/-}$ background. Relative to $p53^{-/-}$ animals, $p53^{+/-}$ mice develop tumors with significantly delayed kinetics and typically display a more diverse tumor spectrum (16, 17, 25). Similar to the results with $p53^{-/-}$ mice, reduced *Hus1* gene dosage did not significantly alter tumor development in $p53^{+/-}$ mice (Fig. 7B). The kinetics of tumor development were actually slightly delayed in mice with reduced Hus1 expression (median survival of 490, 504, 571, and 508 days for $Hus1^{+/+}p53^{-/-}$, $Hus1^{+/neo}p53^{-/-}$, $Hus1^{+/\Delta 1}p53^{-/-}$, and $Hus1^{neo/\Delta 1}p53^{-/-}$ mice, respectively), but these differences were not statistically significant ($P = 0.531$ [log rank test]). Likewise, the distribution of tumor types in $p53^{+/-}$ mice did not vary significantly by *Hus1* genotype ($P = 0.456$ [chi-square test]). Taken together, the analysis of mice with reduced *Hus1* expression suggests that partial *Hus1* impairment, alone or in combination with targeted *p53* inactivation, does not promote tumor development.

DISCUSSION

A full understanding of the physiological functions of the mammalian cell cycle checkpoint pathway involving Atr, Chk1, and the 9-1-1 complex has been elusive in part because complete inactivation of *Hus1* or other components of this pathway in mice causes embryonic lethality. In this report, we describe

FIG. 5. Defective responses to DNA damage and replication blockage in cells expressing reduced levels of *Hus1*. (A) Cell viability following BPDE treatment. $Hus1^{+/\Delta 1}$, $Hus1^{neo/neo}$, and $Hus1^{neo/\Delta 1}$ MEFs at passage one were treated with BPDE, and cell viability was measured 72 h posttreatment. The percentage of viable cells, relative to mock-treated control cultures, is plotted. Values are the mean of triplicate samples, with error bars representing the standard deviation. (B) DNA synthesis following BPDE treatment. $Hus1^{+/\Delta 1}$, $Hus1^{neo/neo}$, and $Hus1^{neo/\Delta 1}$ MEFs at passage two were treated with BPDE and then assayed for DNA synthesis 1 h later by measurement of radiolabeled thymidine incorporation. The percentage of DNA synthesis, relative to that for matched mock-treated control cells, is shown. Values are the mean of triplicate samples, with error bars representing the standard deviation. (C) Cell viability following aphidicolin treatment. $Hus1^{+/\Delta 1}$, $Hus1^{neo/neo}$, and $Hus1^{neo/\Delta 1}$ MEFs at passage one were treated with aphidicolin for 24 h, and cell viability was measured 72 h posttreatment. The percentage of viable cells, relative to mock-treated control cultures, is plotted. Values are the mean of triplicate samples, with error bars representing the standard deviation. (D) γ-H2AX accumulation following aphidicolin treatment. $Hus1^{+/+}$, $Hus1^{neo/neo}$, and $Hus1^{neo/\Delta 1}$ cells at passage three were treated with 0.1 μM aphidicolin for 24 h, and the percentage of γ-H2AX-positive cells was then determined by indirect immunofluorescence. Values are the mean for three independent 40× microscope fields, with error bars representing the standard deviation. (E) Representative metaphase spreads from aphidicolin-treated MEFs. $Hus1^{+/+}$ and $Hus1^{neo/\Delta 1}$ MEFs at passage two were mock treated or treated with 0.1 μM aphidicolin for 24 h. Metaphase spreads were then prepared, stained with Giemsa, and imaged with a 100× objective lens. Thin arrows indicate chromosome gaps and breaks, while thick arrows indicate chromatid interchanges.

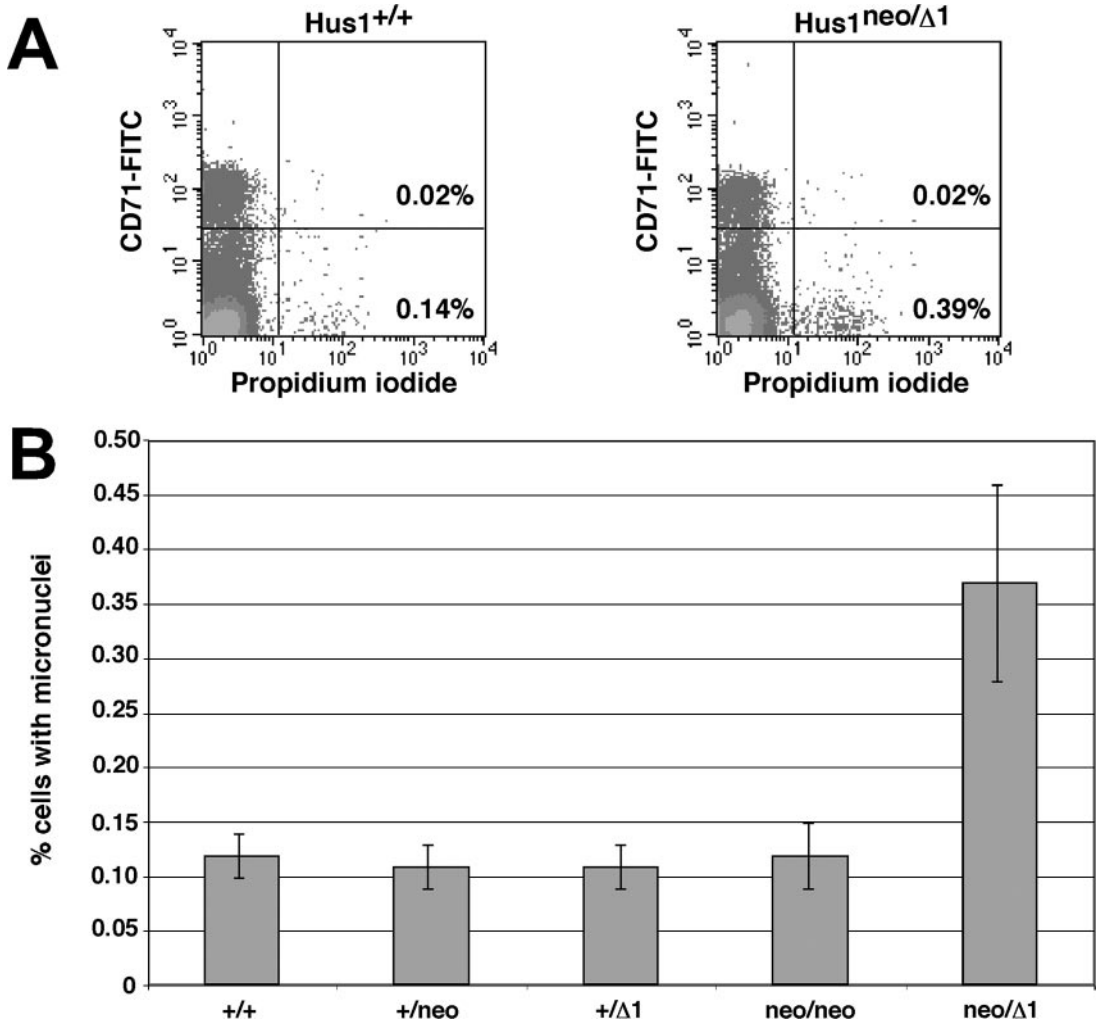

FIG. 6. Increased micronucleus formation in peripheral blood cells from mice with reduced *Hus1* expression. (A) Representative FACS plots. Peripheral blood was drawn from mice of the indicated genotypes, stained with anti-CD71 antibody and propidium iodide, and analyzed by flow cytometry. The lower right quadrant contains mature normochromatic erythrocytes harboring micronuclei. The upper right quadrant contains reticulocytes with micronuclei. (B) Summary of micronucleus formation in peripheral blood from mice of the *Hus1* allelic series. The mean frequency of micronucleus-containing erythrocytes is graphed for $Hus1^{+/+}$ ($n = 5$), $Hus1^{+/neo}$ ($n = 6$), $Hus1^{+/\Delta 1}$ ($n = 6$), $Hus1^{neo/neo}$ ($n = 3$), or $Hus1^{neo/\Delta 1}$ ($n = 10$) female mice, with error bars representing the standard deviation.

a system for assessing the functional consequences of partial impairment of the Hus1-dependent cell cycle checkpoint pathway. This new mouse model centers on a hypomorphic allele, $Hus1^{neo}$, that expresses wild-type *Hus1* transcripts at a reduced level as well as aberrant transcripts with minimal coding capacity. A *Hus1* allelic series was generated by combining this and other *Hus1* alleles. Analysis of the allelic series in cells and mice indicated that *Hus1* gene dosage has a significant impact on genomic integrity during normal growth conditions and in response to DNA damage and further identified an essential role for Hus1 in the maintenance of genomic stability in adult mice. Interestingly, however, mice with reduced *Hus1* expression developed normally and were not tumor prone.

$Hus1^{neo/\Delta 1}$ MEFs underwent premature senescence, whereas cells with a slightly greater level of *Hus1* expression ($Hus1^{neo/neo}$) were capable of normal proliferation. The senescence of cultured mouse cells is believed to reflect a DNA damage response to stressful culture conditions and to be independent of telomere shortening (24). That $Hus1^{neo/\Delta 1}$ cells underwent premature senescence in culture while mice of the same genotype were born at the expected frequency suggests that some aspect of in vitro culture creates a requirement for an intact checkpoint apparatus. The MEFs described here were cultured under atmospheric oxygen levels (~20% oxygen), and others have found that this high oxygen level causes DNA damage that contributes to the senescence of wild-type MEFs (38). During embryonic development, on the other hand, $Hus1^{neo/\Delta 1}$ cells experience lower, physiological oxygen levels and under these conditions the level of *Hus1* expressed from $Hus1^{neo}$ is sufficient for apparently normal proliferation and differentiation. Thus, the partial *Hus1* impairment in $Hus1^{neo/\Delta 1}$ MEFs might trigger premature senescence by sensitizing cells to oxidative stress. Consistent with this possibility, treatment of $Hus1^{neo/\Delta 1}$ cultures with the antioxidant NAC

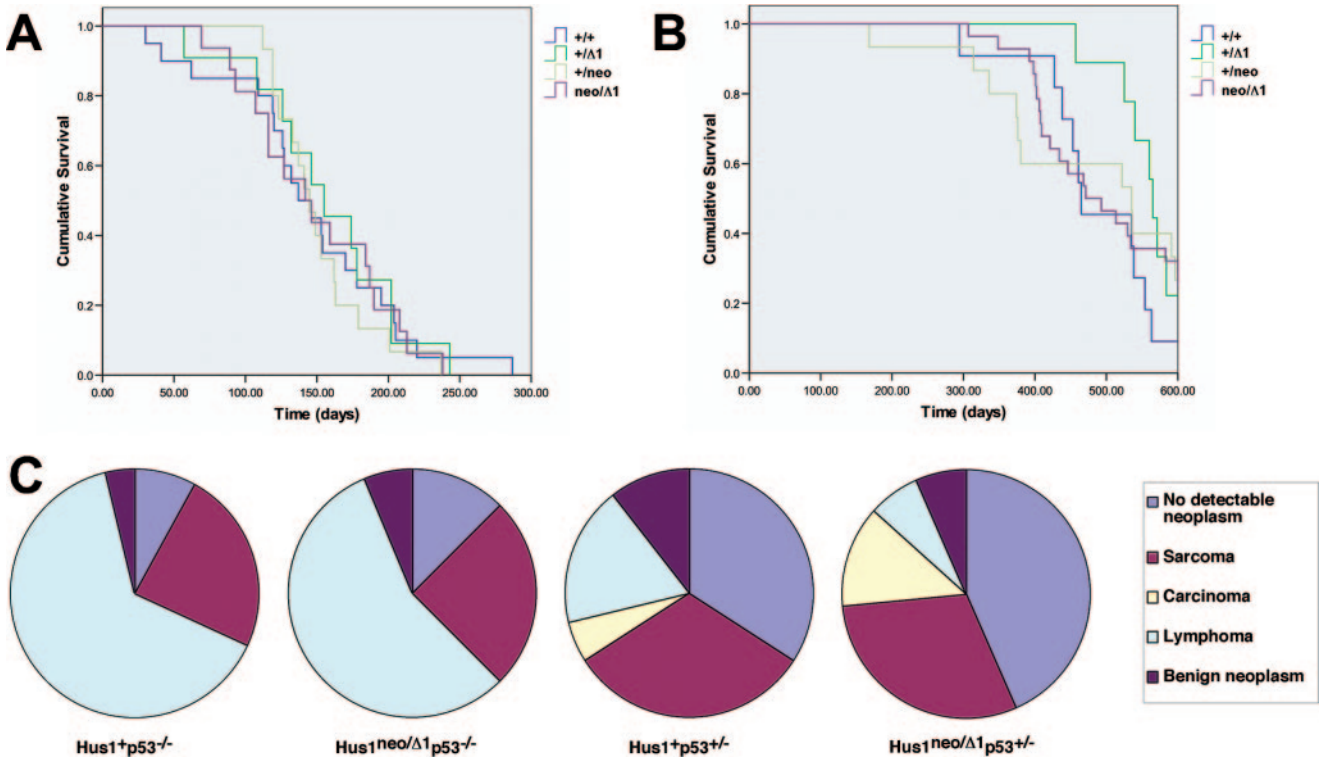

FIG. 7. Partial *Hus1* impairment does not accelerate tumorigenesis or alter the tumor spectrum in $p53^{+/-}$ or $p53^{-/-}$ mice. Survival curves for mice of the indicated *Hus1* genotypes in $p53^{-/-}$ (A) or $p53^{+/-}$ (B) backgrounds. The following number of animals was analyzed for each genotype: $Hus1^{+/+}p53^{-/-}$, 20; $Hus1^{+/neo}p53^{-/-}$, 15; $Hus1^{+/\Delta1}p53^{-/-}$, 11; $Hus1^{neo/\Delta1}p53^{-/-}$, 16; $Hus1^{+/+}p53^{+/-}$, 11; $Hus1^{+/neo}p53^{+/-}$, 15; $Hus1^{+/\Delta1}p53^{+/-}$, 9; $Hus1^{neo/\Delta1}p53^{+/-}$, 28. (C) Pie charts showing the tumor spectrum for the mice described above at the conclusion of the experiment. $Hus1^{+}p53^{-/-}$ and $Hus1^{+}p53^{+/-}$ charts include the combined results for $Hus1^{+/+}$, $Hus1^{+/neo}$, and $Hus1^{+/\Delta1}$ mice. Hematoxylin- and eosin-stained tissue sections prepared from necropsied mice were analyzed blind with respect to genotype, and tumors were categorized as sarcoma, carcinoma, lymphoma and other hematopoietic neoplasms, or benign neoplasms. "No detectable neoplasm" refers to mice that remained healthy at the completion of the experiment or for which no neoplasm was identified at necropsy.

largely suppressed the premature senescence phenotype. The improved proliferation of $Hus1^{neo/\Delta1}$ cells following antioxidant treatment was associated with a significant reduction in the frequency of spontaneous chromosomal abnormalities (data not shown). It is worth noting that the 9-1-1 checkpoint complex associates with a number of proteins required for base excision repair, the DNA repair pathway that mediates many of the responses to oxidative DNA damage (10, 20, 48, 55, 58, 59). These findings suggest that an essential function of the 9-1-1 complex during an unperturbed cell cycle is responding to spontaneous oxidative DNA lesions.

Analysis of the *Hus1* allelic series also revealed how incremental reductions in *Hus1* expression affect responses to extrinsic genotoxins. $Hus1^{neo/\Delta1}$ MEFs were found to be hypersensitive to both DNA damaging agents and replication inhibitors. An intermediate level of genotoxin sensitivity was observed for $Hus1^{neo/neo}$ MEFs, even though untreated cells of this genotype were fully capable of normal proliferation. This suggests that the level of Hus1 in $Hus1^{neo/neo}$ MEFs is sufficient for the response to intrinsic cellular stresses but is sublimiting upon additional genome damage. Importantly, increasing *Hus1* expression via a *Hus1*-expressing retrovirus restored normal genotoxin sensitivity to both $Hus1^{neo/neo}$ and $Hus1^{neo/\Delta1}$ MEFs (data not shown). Consistent with our previous results (64), the sensitivity of cells with reduced *Hus1* expression to the DNA adducting agent BPDE roughly correlated with the functioning of an intra-S cell cycle checkpoint mechanism that represses DNA synthesis following DNA damage. Sensitivity to the replication inhibitor aphidicolin was associated with increased DSB formation, as indicated by increased H2AX phosphorylation, as well as increased formation of chromosomal abnormalities. These findings are in accord with current models suggesting that replication stress in checkpoint-defective cells results in replication fork collapse (5). Interestingly, while $Hus1^{+/+}$ cells showed a slight increase in chromosomal gaps and breaks following low-dose aphidicolin treatment, $Hus1^{neo/neo}$ and $Hus1^{neo/\Delta1}$ cells accumulated not only gaps and breaks but also chromatid interchanges at high frequency. This phenotype is somewhat reminiscent of that observed for Fanconi anemia cells following treatment with mitomycin C, which also involves high-frequency radial chromosome formation (13). Genotoxin-induced chromatid interchanges are believed to reflect a failure of DNA repair by homologous recombination and increased use of error-prone pathways such as nonhomologous end joining and single-strand annealing. A similar shift in repair pathway usage might account for the occurrence of certain chromosome aberrations in cells with reduced *Hus1* expression, as mammalian Hus1, Rad9, Rad17, and Chk1 proteins are required for homologous recombinational repair (7, 37, 49, 61) and the yeast 9-1-1 complex has been implicated in translesion DNA synthesis (26, 42).

Consistent with the observed increase in chromosomal abnormalities in *Hus1*$^{neo/\Delta 1}$ MEFs, peripheral blood cells from *Hus1*$^{neo/\Delta 1}$ mice showed increased micronucleus formation. It is important to note that the micronucleus frequency measurements gauge genomic instability specifically in red blood cell precursors, and the extent of genomic instability in other tissues of *Hus1*$^{neo/\Delta 1}$ mice remains unknown. Nevertheless, despite this indicator of genomic instability, *Hus1*$^{neo/\Delta 1}$ mice were not predisposed to spontaneous tumor development. Furthermore, reduced *Hus1* expression did not affect the kinetics of tumor development in *p53*$^{+/-}$ or *p53*$^{-/-}$ mice or significantly change the spectrum of tumors arising in these animals. Several other mouse models featuring defects in cell cycle checkpoints and/or DNA repair similarly do not show increased cancer incidence (1, 13, 47, 52, 66). These data contribute to the emerging picture that a particular type and level of genomic instability may be critical to tumor development (9). In the case of *Hus1*$^{neo/\Delta 1}$ mice, the frequency of cancer-inducing chromosomal abnormalities may be too low or, alternatively, genetically unstable preneoplastic cells with reduced *Hus1* expression may be incapable of extensive proliferation, as suggested by their propensity to undergo premature senescence in culture. One interesting possibility is that the low level of genome damage in *Hus1*$^{neo/\Delta 1}$ mice could accumulate over multiple generations. We have interbred *Hus1*$^{neo/\Delta 1}$ mice for over five generations and continue to obtain viable, fertile *Hus1*$^{neo/\Delta 1}$ offspring. Whether these animals will develop late-onset phenotypes remains to be determined.

While cell cycle checkpoints in general are key tumor suppressor mechanisms (3, 21, 27), the available evidence suggests that defects in the Atr-dependent checkpoint mechanism may not strongly promote tumorigenesis. In mammals, the components of this pathway are essential, and their complete inactivation may not be compatible with tumor cell proliferation. *Chk1*$^{+/-}$ mice are not prone to spontaneous tumor development (31), and only a slight tumor predisposition is seen for *Atr*$^{+/-}$ mice (6). Consistent with these animal studies, there are only limited reports of *ATR* and *CHK1* mutations in human cancers (32, 56) and it is uncertain whether these mutations are causative. Seckel syndrome, caused by a hypomorphic *ATR* mutation, is primarily a developmental disorder that has not been associated with increased tumor predisposition, although relatively few patients have been analyzed (35). However, heterozygosity for *Chk1* does accelerate *Wnt1*-induced mammary tumorigenesis to a limited extent (31), while *Atr* heterozygosity increases tumor frequency in mismatch repair-defective mice (18). Thus, it may be that only very specific hypomorphic mutations affecting this pathway, in particular genetic or environmental contexts, will stimulate oncogenesis. Further analysis of the mice described here should provide additional insights into possible tumor suppressor functions for Hus1 and further clarify the impact of checkpoint defects and genomic instability on cancer initiation and progression.

ACKNOWLEDGMENTS

We thank Naoko Shima for advice on micronucleus formation assays; Francoise Vermeylen, of the Cornell Statistical Consulting Unit, for advice on statistical analyses; Young Lu and Rinti Mukherjee for assistance with data processing; Fei Sun for performing preliminary antioxidant treatment experiments; the staff of the Cornell Center for Animal Resources and Education (CARE) and Lab Animal Services for excellent animal care; and Cyrus Vaziri, Tom Wolkow, and members of the Weiss lab for helpful discussion and comments on the manuscript.

This work was supported by NIH grant R01 CA108773 (R.S.W.). A.C. was supported in part through the Cornell University Veterinary Investigator Program, and J.D. was a participant in the Lansing High School Authentic Scientific Research Program.

REFERENCES

1. **Baker, D. J., K. B. Jeganathan, J. D. Cameron, M. Thompson, S. Juneja, A. Kopecka, R. Kumar, R. B. Jenkins, P. C. de Groen, P. Roche, and J. M. van Deursen.** 2004. BubR1 insufficiency causes early onset of aging-associated phenotypes and infertility in mice. Nat. Genet. **36:**744–749.
2. **Bao, S., T. Lu, X. Wang, H. Zheng, L. E. Wang, Q. Wei, W. N. Hittelman, and L. Li.** 2004. Disruption of the Rad9/Rad1/Hus1 (9-1-1) complex leads to checkpoint signaling and replication defects. Oncogene **23:**5586–5593.
3. **Bartkova, J., Z. Horejsi, K. Koed, A. Kramer, F. Tort, K. Zieger, P. Guldberg, M. Sehested, J. M. Nesland, C. Lukas, T. Orntoft, J. Lukas, and J. Bartek.** 2005. DNA damage response as a candidate anti-cancer barrier in early human tumorigenesis. Nature **434:**864–870.
4. **Blasco, M. A., H. W. Lee, M. P. Hande, E. Samper, P. M. Lansdorp, R. A. DePinho, and C. W. Greider.** 1997. Telomere shortening and tumor formation by mouse cells lacking telomerase RNA. Cell **91:**25–34.
5. **Branzei, D., and M. Foiani.** 2005. The DNA damage response during DNA replication. Curr. Opin. Cell Biol. **17:**568–575.
6. **Brown, E. J., and D. Baltimore.** 2000. *ATR* disruption leads to chromosomal fragmentation and early embryonic lethality. Genes Dev. **14:**397–402.
7. **Budzowska, M., I. Jaspers, J. Essers, H. De Waard, E. Van Drunen, K. Hanada, B. Beverloo, R. W. Hendriks, A. De Klein, R. Kanaar, J. H. Hoeijmakers, and A. Maas.** 2004. Mutation of the mouse Rad17 gene leads to embryonic lethality and reveals a role in DNA damage-dependent recombination. EMBO J. **23:**3548–3558.
8. **Burtelow, M. A., S. H. Kaufmann, and L. M. Karnitz.** 2000. Retention of the human Rad9 checkpoint complex in extraction-resistant nuclear complexes after DNA damage. J. Biol. Chem. **275:**26343–26348.
9. **Cahill, D. P., K. W. Kinzler, B. Vogelstein, and C. Lengauer.** 1999. Genetic instability and Darwinian selection in tumours. Trends Cell Biol. **9:**M57–60.
10. **Chang, D. Y., and A. L. Lu.** 2005. Interaction of checkpoint proteins Hus1/Rad1/Rad9 with DNA base excision repair enzyme MutY homolog in fission yeast, Schizosaccharomyces pombe. J. Biol. Chem. **280:**408–417.
11. **Cimprich, K. A.** 2003. Fragile sites: breaking up over a slowdown. Curr. Biol. **13:**R231–R233.
12. **Cortez, D.** 2005. Unwind and slow down: checkpoint activation by helicase and polymerase uncoupling. Genes Dev. **19:**1007–1012.
13. **D'Andrea, A. D.** 2003. The Fanconi road to cancer. Genes Dev. **17:**1933–1936.
14. **de Klein, A., M. Muijtjens, R. van Os, Y. Verhoeven, B. Smit, A. M. Carr, A. R. Lehmann, and J. H. Hoeijmakers.** 2000. Targeted disruption of the cell-cycle checkpoint gene *ATR* leads to early embryonic lethality in mice. Curr. Biol. **10:**479–482.
15. **Dertinger, S. D., D. K. Torous, and K. R. Tometsko.** 1996. Simple and reliable enumeration of micronucleated reticulocytes with a single-laser flow cytometer. Mutat. Res. **371:**283–292.
16. **Donehower, L. A., M. Harvey, B. L. Slagle, M. J. McArthur, C. A. J. Montgomery, J. S. Butel, and A. Bradley.** 1992. Mice deficient for p53 are developmentally normal but susceptible to spontaneous tumours. Nature **356:**215–221.
17. **Donehower, L. A., M. Harvey, H. Vogel, M. J. McArthur, C. A. Montgomery, Jr., S. H. Park, T. Thompson, R. J. Ford, and A. Bradley.** 1995. Effects of genetic background on tumorigenesis in p53-deficient mice. Mol. Carcinog. **14:**16–22.
18. **Fang, Y., C. C. Tsao, B. K. Goodman, R. Furumai, C. A. Tirado, R. T. Abraham, and X. F. Wang.** 2004. ATR functions as a gene dosage-dependent tumor suppressor on a mismatch repair-deficient background. EMBO J. **23:**3164–3174.
19. **Francia, S., R. S. Weiss, M. P. Hande, R. Freire, and F. d'Adda di Fagagna.** 2006. Telomere and telomerase modulation by the mammalian Rad9/Rad1/Hus1 DNA-damage-checkpoint complex. Curr. Biol. **16:**1551–1558.
20. **Friedrich-Heineken, E., M. Toueille, B. Tannler, C. Burki, E. Ferrari, M. O. Hottiger, and U. Hubscher.** 2005. The two DNA clamps Rad9/Rad1/Hus1 complex and proliferating cell nuclear antigen differentially regulate flap endonuclease 1 activity. J. Mol. Biol. **353:**980–989.
21. **Gorgoulis, V. G., L. V. Vassiliou, P. Karakaidos, P. Zacharatos, A. Kotsinas, T. Liloglou, M. Venere, R. A. Ditullio, Jr., N. G. Kastrinakis, B. Levy, D. Kletsas, A. Yoneta, M. Herlyn, C. Kittas, and T. D. Halazonetis.** 2005. Activation of the DNA damage checkpoint and genomic instability in human precancerous lesions. Nature **434:**907–913.
22. **Heddle, J. A., M. C. Cimino, M. Hayashi, F. Romagna, M. D. Shelby, J. D. Tucker, P. Vanparys, and J. T. MacGregor.** 1991. Micronuclei as an index of cytogenetic damage: past, present, and future. Environ. Mol. Mutagen. **18:**277–291.

23. **Hopkins, K. M., W. Auerbach, X. Y. Wang, M. P. Hande, H. Hang, D. J. Wolgemuth, A. L. Joyner, and H. B. Lieberman.** 2004. Deletion of mouse *Rad9* causes abnormal cellular responses to DNA damage, genomic instability, and embryonic lethality. Mol. Cell. Biol. **24:**7235–7248.
24. **Itahana, K., J. Campisi, and G. P. Dimri.** 2004. Mechanisms of cellular senescence in human and mouse cells. Biogerontology **5:**1–10.
25. **Jacks, T., L. Remington, B. O. Williams, E. M. Schmitt, S. Halachmi, R. T. Bronson, and R. A. Weinberg.** 1994. Tumor spectrum analysis in p53-mutant mice. Curr. Biol. **4:**1–7.
26. **Kai, M., and T. S. Wang.** 2003. Checkpoint activation regulates mutagenic translesion synthesis. Genes Dev. **17:**64–76.
27. **Kastan, M. B., and J. Bartek.** 2004. Cell-cycle checkpoints and cancer. Nature **432:**316–323.
28. **Kinzel, B., J. Hall, F. Natt, J. Weiler, and D. Cohen.** 2002. Downregulation of Hus1 by antisense oligonucleotides enhances the sensitivity of human lung carcinoma cells to cisplatin. Cancer **94:**1808–1814.
29. **Kwan, K. M.** 2002. Conditional alleles in mice: practical considerations for tissue-specific knockouts. Genesis **32:**49–62.
30. **Levitt, P. S., H. Liu, C. Manning, and R. S. Weiss.** 2005. Conditional inactivation of the mouse Hus1 cell cycle checkpoint gene. Genomics **86:**212–224.
31. **Liu, Q., S. Guntuku, X. S. Cui, S. Matsuoka, D. Cortez, K. Tamai, G. Luo, S. Carattini-Rivera, F. DeMayo, A. Bradley, L. A. Donehower, and S. J. Elledge.** 2000. Chk1 is an essential kinase that is regulated by Atr and required for the G_2/M DNA damage checkpoint. Genes Dev. **14:**1448–1459.
32. **Menoyo, A., H. Alazzouzi, E. Espin, M. Armengol, H. Yamamoto, and S. Schwartz, Jr.** 2001. Somatic mutations in the DNA damage-response genes ATR and CHK1 in sporadic stomach tumors with microsatellite instability. Cancer Res. **61:**7727–7730.
33. **Meyers, E. N., M. Lewandoski, and G. R. Martin.** 1998. An Fgf8 mutant allelic series generated by Cre- and Flp-mediated recombination. Nat. Genet. **18:**136–141.
34. **Mitelman, F. (ed.).** 1995. ISCN (1995): an international system for human cytogenetic nomenclature. S. Karger, Basel, Switzerland.
35. **O'Driscoll, M., A. R. Gennery, J. Seidel, P. Concannon, and P. A. Jeggo.** 2004. An overview of three new disorders associated with genetic instability: LIG4 syndrome, RS-SCID and ATR-Seckel syndrome. DNA Repair **3:**1227–1235.
36. **O'Driscoll, M., V. L. Ruiz-Perez, C. G. Woods, P. A. Jeggo, and J. A. Goodship.** 2003. A splicing mutation affecting expression of ataxia-telangiectasia and Rad3-related protein (ATR) results in Seckel syndrome. Nat. Genet. **33:**497–501.
37. **Pandita, R. K., G. G. Sharma, A. Laszlo, K. M. Hopkins, S. Davey, M. Chakhparonian, A. Gupta, R. J. Wellinger, J. Zhang, S. N. Powell, J. L. Roti Roti, H. B. Lieberman, and T. K. Pandita.** 2006. Mammalian Rad9 plays a role in telomere stability, S- and G_2-phase-specific cell survival, and homologous recombinational repair. Mol. Cell. Biol. **26:**1850–1864.
38. **Parrinello, S., E. Samper, A. Krtolica, J. Goldstein, S. Melov, and J. Campisi.** 2003. Oxygen sensitivity severely limits the replicative lifespan of murine fibroblasts. Nat. Cell Biol. **5:**741–747.
39. **Reinholdt, L., T. Ashley, J. Schimenti, and N. Shima.** 2004. Forward genetic screens for meiotic and mitotic recombination-defective mutants in mice. Methods Mol. Biol. **262:**87–107.
40. **Roos-Mattjus, P., K. M. Hopkins, A. J. Oestreich, B. T. Vroman, K. L. Johnson, S. Naylor, H. B. Lieberman, and L. M. Karnitz.** 2003. Phosphorylation of human Rad9 is required for genotoxin-activated checkpoint signaling. J. Biol. Chem. **278:**24428–24437.
41. **Roos-Mattjus, P., B. T. Vroman, M. A. Burtelow, M. Rauen, A. K. Eapen, and L. M. Karnitz.** 2002. Genotoxin-induced Rad9-Hus1-Rad1 (9-1-1) chromatin association is an early checkpoint signaling event. J. Biol. Chem. **277:**43809–43812.
42. **Sabbioneda, S., B. K. Minesinger, M. Giannattasio, P. Plevani, M. Muzi-Falconi, and S. Jinks-Robertson.** 2005. The 9-1-1 checkpoint clamp physically interacts with polζ and is partially required for spontaneous polζ-dependent mutagenesis in *Saccharomyces cerevisiae*. J. Biol. Chem. **280:**38657–38665.
43. **Savage, J. R.** 1976. Classification and relationships of induced chromosomal structural changes. J. Med. Genet. **13:**103–122.
44. **Shechter, D., V. Costanzo, and J. Gautier.** 2004. Regulation of DNA replication by ATR: signaling in response to DNA intermediates. DNA Repair **3:**901–908.
45. **Shechter, D., and J. Gautier.** 2005. ATM and ATR check in on origins: a dynamic model for origin selection and activation. Cell Cycle **4:**e74–e77.
46. **Shi, G., D. Y. Chang, C. C. Cheng, X. Guan, C. Venclovas, and A. L. Lu.** 2006. Physical and functional interactions between MutY homolog (MYH) and checkpoint proteins Rad9-Rad1-Hus1. Biochem. J. **400:**53–62.
47. **Shima, N., R. J. Munroe, and J. C. Schimenti.** 2004. The mouse genomic instability mutation *chaos1* is an allele of *Polq* that exhibits genetic interaction with *Atm*. Mol. Cell. Biol. **24:**10381–10389.
48. **Smirnova, E., M. Toueille, E. Markkanen, and U. Hubscher.** 2005. The human checkpoint sensor and alternative DNA clamp Rad9-Rad1-Hus1 modulates the activity of DNA ligase I, a component of the long-patch base excision repair machinery. Biochem. J. **389:**13–17.
49. **Sorensen, C. S., L. T. Hansen, J. Dziegielewski, R. G. Syljuasen, C. Lundin, J. Bartek, and T. Helleday.** 2005. The cell-cycle checkpoint kinase Chk1 is required for mammalian homologous recombination repair. Nat. Cell Biol. **7:**195–201.
50. **Sorensen, C. S., R. G. Syljuasen, J. Lukas, and J. Bartek.** 2004. ATR, Claspin and the Rad9-Rad1-Hus1 complex regulate Chk1 and Cdc25A in the absence of DNA damage. Cell Cycle **3:**941–945.
51. **Takai, H., K. Tominaga, N. Motoyama, Y. A. Minamishima, H. Nagahama, T. Tsukiyama, K. Ikeda, K. Nakayama, M. Nakanishi, and K. Nakayama.** 2000. Aberrant cell cycle checkpoint function and early embryonic death in *Chk1*$^{-/-}$ mice. Genes Dev. **14:**1439–1447.
52. **Theunissen, J. W., M. I. Kaplan, P. A. Hunt, B. R. Williams, D. O. Ferguson, F. W. Alt, and J. H. Petrini.** 2003. Checkpoint failure and chromosomal instability without lymphomagenesis in Mre11(ATLD1/ATLD1) mice. Mol. Cell **12:**1511–1523.
53. **Thiriet, C., and J. J. Hayes.** 2005. Chromatin in need of a fix: phosphorylation of H2AX connects chromatin to DNA repair. Mol. Cell **18:**617–622.
54. **Todaro, G. J., and H. Green.** 1963. Quantitative studies of the growth of mouse embryo cells in culture and their development into established lines. J. Cell Biol. **17:**299–313.
55. **Toueille, M., N. El-Andaloussi, I. Frouin, R. Freire, D. Funk, I. Shevelev, E. Friedrich-Heineken, G. Villani, M. O. Hottiger, and U. Hubscher.** 2004. The human Rad9/Rad1/Hus1 damage sensor clamp interacts with DNA polymerase beta and increases its DNA substrate utilisation efficiency: implications for DNA repair. Nucleic Acids Res. **32:**3316–3324.
56. **Vassileva, V., A. Millar, L. Briollais, W. Chapman, and B. Bapat.** 2002. Genes involved in DNA repair are mutational targets in endometrial cancers with microsatellite instability. Cancer Res. **62:**4095–4099.
57. **Venclovas, C., and M. P. Thelen.** 2000. Structure-based predictions of Rad1, Rad9, Hus1 and Rad17 participation in sliding clamp and clamp-loading complexes. Nucleic Acids Res. **28:**2481–2493.
58. **Wang, W., P. Brandt, M. L. Rossi, L. Lindsey-Boltz, V. Podust, E. Fanning, A. Sancar, and R. A. Bambara.** 2004. The human Rad9-Rad1-Hus1 checkpoint complex stimulates flap endonuclease 1. Proc. Natl. Acad. Sci. USA **101:**16762–16767.
59. **Wang, W., L. A. Lindsey-Boltz, A. Sancar, and R. A. Bambara.** 2006. Mechanism of stimulation of human DNA ligase I by the Rad9-Rad1-Hus1 checkpoint complex. J. Biol. Chem. **281:**20865–20872.
60. **Wang, X., J. Guan, B. Hu, R. S. Weiss, G. Iliakis, and Y. Wang.** 2004. Involvement of Hus1 in the chain elongation step of DNA replication after exposure to camptothecin or ionizing radiation. Nucleic Acids Res. **32:**767–775.
61. **Wang, X., B. Hu, R. S. Weiss, and Y. Wang.** 2006. The effect of Hus1 on ionizing radiation sensitivity is associated with homologous recombination repair but is independent of nonhomologous end-joining. Oncogene **25:**1980–1983.
62. **Ward, I. M., and J. Chen.** 2001. Histone H2AX is phosphorylated in an ATR-dependent manner in response to replicational stress. J. Biol. Chem. **276:**47759–47762.
63. **Weiss, R. S., T. Enoch, and P. Leder.** 2000. Inactivation of mouse *Hus1* results in genomic instability and impaired responses to genotoxic stress. Genes Dev. **14:**1886–1898.
64. **Weiss, R. S., P. Leder, and C. Vaziri.** 2003. Critical role for mouse Hus1 in an S-phase DNA damage cell cycle checkpoint. Mol. Cell. Biol. **23:**791–803.
65. **Weiss, R. S., S. Matsuoka, S. J. Elledge, and P. Leder.** 2002. Hus1 acts upstream of Chk1 in a mammalian DNA damage response pathway. Curr. Biol. **12:**73–77.
66. **Williams, B. R., O. K. Mirzoeva, W. F. Morgan, J. Lin, W. Dunnick, and J. H. Petrini.** 2002. A murine model of Nijmegen breakage syndrome. Curr. Biol. **12:**648–653.
67. **Zou, L., D. Cortez, and S. J. Elledge.** 2002. Regulation of ATR substrate selection by Rad17-dependent loading of Rad9 complexes onto chromatin. Genes Dev. **16:**198–208.